

Strategies for computing the scalar self-force on a Schwarzschild background

Steven Dorsher

Louisiana State University

September 26, 2017

Gravitational Waves

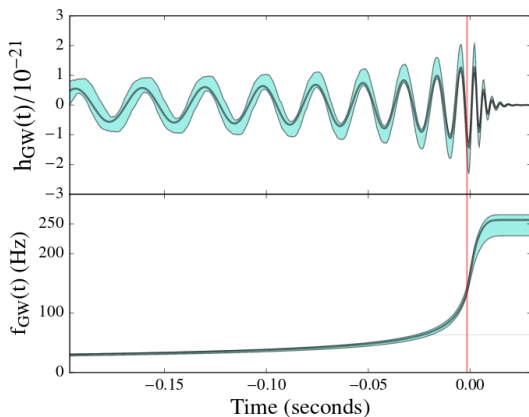
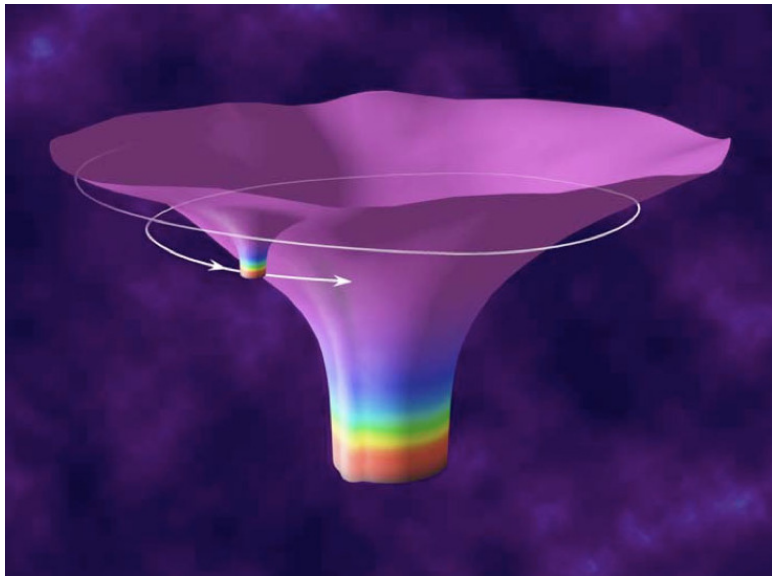


Figure: LIGO detection, September 14, 2015. General relativity was tested by comparing inspiral with merger/ringdown phases.

Extreme Mass Ratio Inspirals



Laser Interferometer Space Antenna

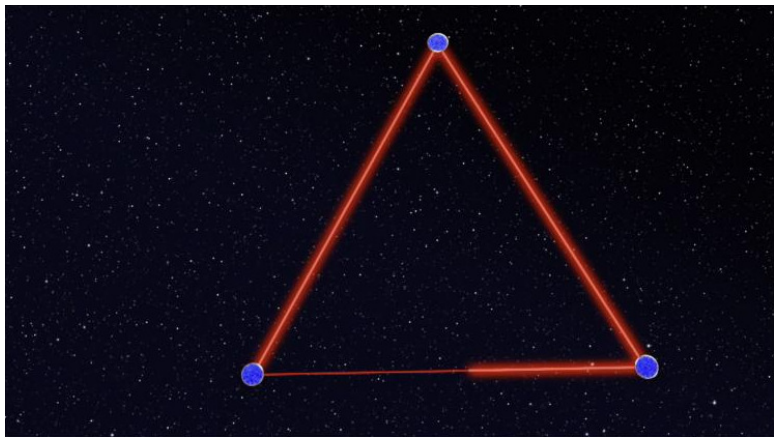


Figure: Laser Interferometer Space Antenna, which will operate around launches in early 2030's, ESA-NASA partnership, will detect EMRI's

Toward LISA EMRI templates

- ▶ Generating LISA EMRI templates require evolving 10^6 orbits with precision on the order of $\delta P/P \sim 10^{-6}$ *Danzmann, Karsten. LISA: A proposal in response to the ESA call for L3 mission concepts (2017)*
- ▶ For EMRI's, the self-force approximation is used in the limit where the mass ratio is large (10^4 to 10^6)
- ▶ EMRI's have an orbital evolution timescale that scales as M/μ , and a period that scales as M . These two widely different timescales necessitate a different numerical approach than numerical relativity.
- ▶ Self-force prescribes a perturbative approximation in the mass ratio.

Self-force in general relativity

- ▶ In general relativity, test particles move along geodesics
- ▶ A compact object is not a test particle
- ▶ Motion \rightarrow radiation \rightarrow energy and angular momentum loss \rightarrow inspiral
- ▶ Applies to scalar, electromagnetic, and tensor fields on a gravitational background
- ▶ Perturbative expansion in powers of the mass ratio

Goals for the self-force community and this project

The long term goal for the field is to generate extremely precise EMRI gravitational wave templates for LISA.

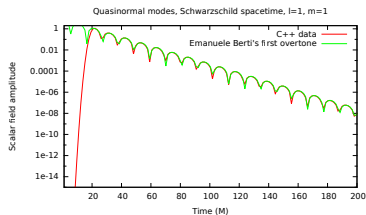
- ▶ Scalar rather than tensor waves (Ψ rather than $h_{\mu\nu}$)
- ▶ Non-rotating black holes: Schwarzschild spacetime
- ▶ Our collaborator Niels Warburton assumes: the particle has been on the same geodesic for all time when he calculates the self-force
- ▶ Geodesic evolution neglects the effect of the self-force on the particle's orbit when computing the self-force— thus, it is not self-consistent.
- ▶ In our self-consistent evolution, our self-force is evolved in the time domain— field itself encodes info about the past

Our goal is to implement a highly accurate self-consistent evolution and do a comparison study with Niels Warburton's geodesic evolution.

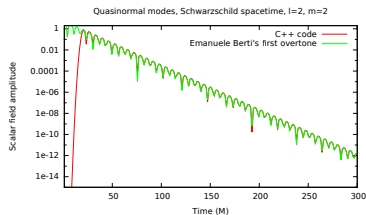
Schwarzschild spacetime without a source

- ▶ Wave equation: $\square\Psi = \frac{1}{\sqrt{-g}}\partial_\mu(g^{\mu\nu}(\partial_\nu\Psi)\sqrt{-g}) = 0$
- ▶ Multipole moment decomposition to account for angular dependence
- ▶ Quasinormal mode (QNM) ringing
 - ▶ higher frequencies and faster decay for higher l
 - ▶ due to interactions near peak of potential
- ▶ Power law tails
 - ▶ go as $t^{-(2l+3)}$
 - ▶ follow the QNM
 - ▶ due to scattering off spacetime far from the peak of the potential

Quasinormal modes



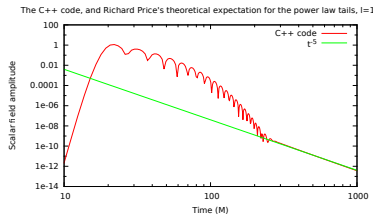
(a) $l = 1$



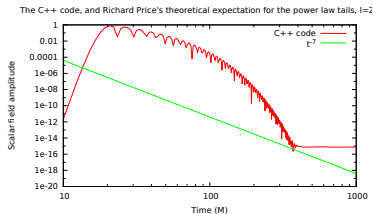
(b) $l = 2$

Figure: $l = 2$ has a higher frequency and a faster decay rate than $l = 1$

Power law tails



(a) $l = 1$



(b) $l = 2$

Figure: $l = 1$ decays as t^{-5} as expected; however, $l = 2$ has no power law tail due to truncation error

The regular and singular field and effective source

- ▶ Regularize field: $\psi^R = \psi^{ret} - \psi^S$
- ▶ Detweiler-Whiting singular field: *Steven Detweiler, Bernard F. Whiting (2002). Phys. Rev. D 67, 024025*
- ▶ $\square\psi^R = S_{eff} = \square\psi^{ret} - \square(W\tilde{\psi}^S)$
- ▶ $\square\psi^{ret} = -4\pi q \int \delta_4(x, z(\tau')) d\tau'$
- ▶ In tensor case for gravitational field, perturbative expansion in terms of powers of radius

Eccentric orbits using Peter Diener's simulation

- ▶ $\chi, \phi \rightarrow$ precession
- ▶ The orbit is artificially held on a geodesic to counteract the self-force generating the scalar waves
- ▶ p, e held fixed, monotonically evolving χ, ϕ
- ▶ $r_{\text{periastron}} = \frac{pM}{1+e}, r_{\text{apastron}} = \frac{pM}{1-e}$
- ▶ Radial self-force: $F_r = q\partial_r\Psi^R$

Self-force spherical harmonic components depend on time

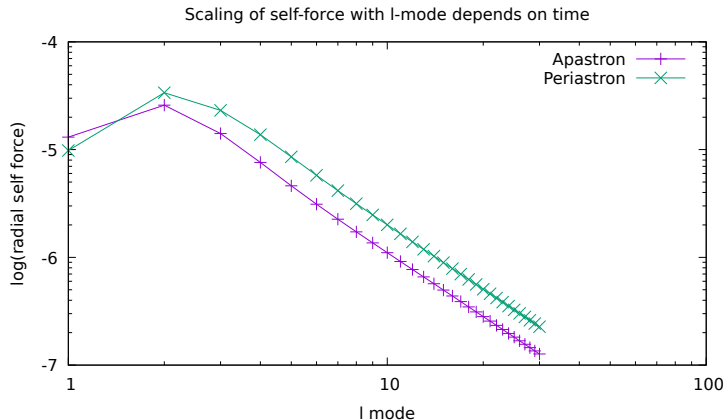


Figure: Periastron has a higher self-force amplitude for nearly every spherical harmonic than apastron.

The first order Richardson extrapolation

- ▶ Discontinuous Galerkin: ODE solver with truncation errors that scale as h^{n+1}
- ▶ Assume $F_r(n, l) = F_{inf}(l) + c(l) \exp(-\alpha n)$
- ▶ Obtain extrapolation by solving system of equations for $F_r(n_i, l)$, $i = 1, 2, 3$

Well-converging data

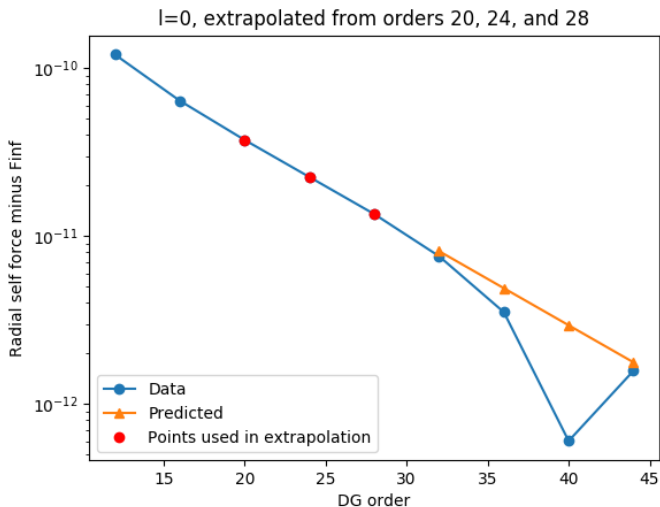


Figure: $l=0$ at $t=370$. This data converges very cleanly until it hits roundoff noise at high DG orders.

Error due to neglecting the first order Richardson extrapolation

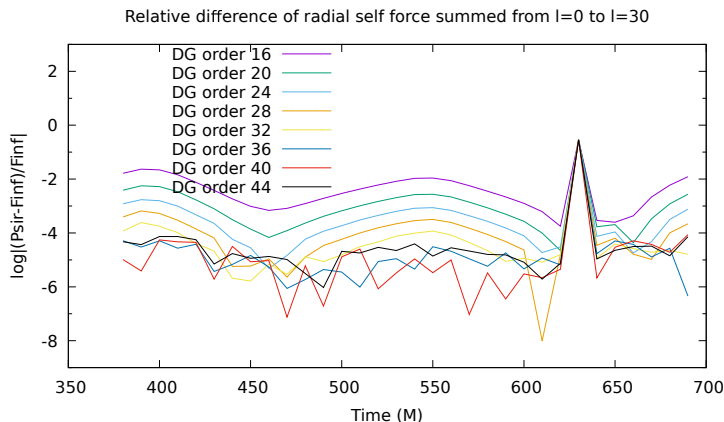


Figure: Relative error between DG starting orders and F_{inf} vs time. For DG order 36 where roundoff error sets in, the error is about 10^{-4} .

The l-mode sum and fit

- ▶ Use spherical harmonic decomposition of Ψ to encode angular information
- ▶ must sum over l and m at end to obtain self force
- ▶ Use fit to extend sum to $l = \infty$

$$F_r(l, t) = \frac{A(t)}{(2l-1)(2l+3)} + \frac{B(t)}{(2l-3)(2l-1)(2l+3)(2l+5)} \\ + \frac{C(t)}{(2l-5)(2l-3)(2l-1)(2l+3)(2l+5)(2l+7)} + \dots \quad (1)$$

Anna Heffernan, Adrian Ottewill, Barry Wardell (2012). Phys. Rev. D 86, 104023

- ▶ Fit from l_{min} to l_{max} .
- ▶ Sum numerically from zero to l_{max} then use fit coefficients to analytically sum to $l = \infty$

l-mode fit

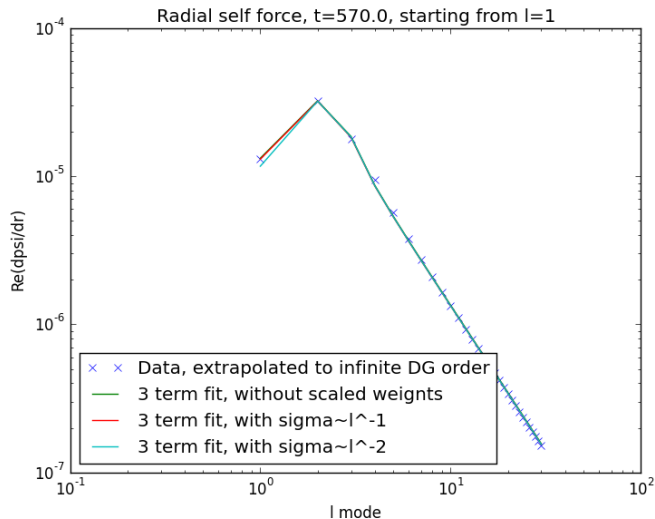


Figure: l -mode versus F_{inf} .

Smooth evolution of total radial self-force

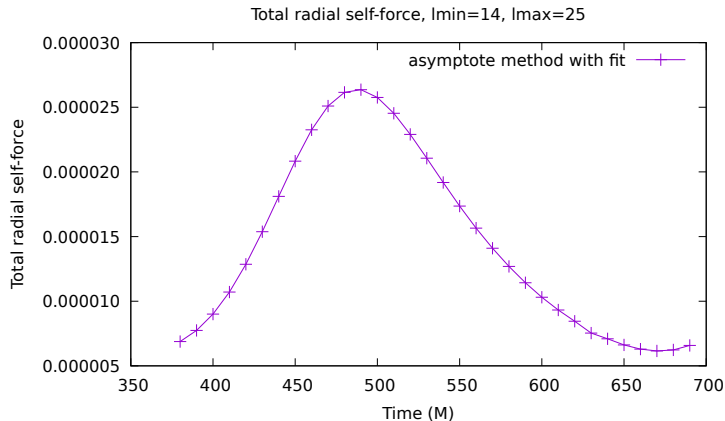


Figure: Total radial self-force including sum to $l = \infty$ over time

Error analysis conclusions

- ▶ The relative error due to neglecting the first order Richardson extrapolation is 10^{-4} . The best order at which to run is DG order 36. Limit dominated by roundoff error.
- ▶ The best $l_{min} = 14$ and $l_{max}=25$. The relative error in these choice of values is 10^{-4} .
- ▶ The relative error due to the number of terms used in the fit is 10^{-4} .
- ▶ The error due to the use of weights in fitting is insignificant.
- ▶ These results are preliminary and need further investigation.

Comparison study of self-consistent to geodesic evolution

- ▶ Self-consistent evolution naturally accounts for the interaction of the particle with the field it has generated in the past since it is evolved in the time domain
 - ▶ The acceleration may need to be taken into account in the effective source
 - ▶ The mass of the particle also evolves according to the work being done on it
 - ▶ Evolved using the osculating orbits framework that slowly evolves p and e and has monotonic χ and ϕ
 - ▶ Capable of evolving to the plunge
- ▶ Geodesic evolution uses a self-force that assumes the particle has been evolving on the same geodesic for all time
 - ▶ Self-force can be efficiently calculated in the frequency domain due to periodicity
 - ▶ Evolves in the time domain after generating the self-force in the frequency domain
 - ▶ Cannot handle effects where the timescale of the orbital evolution is short compared to the period; therefore, cannot evolve to the plunge

Long term goals

- ▶ Goal is to compare Diener's self-consistent code using Warburton's initial conditions and Wardell's effective source to Warburton's geodesic evolutions using frequency domain self force.
- ▶ I will run the simulation, examine physical quantities of interest, and help revise the simulation as necessary.
- ▶ Specifically, it would be interesting to compare the rate of the phase evolution of the self force, since high precision in this quantity is required for LISA detections
- ▶ In particular, some instabilities in the self-consistent evolutions need to be addressed before a publication will be possible. I will help look for a solution to those instabilities.
- ▶ Timescale: highly variable depending upon instabilities. 2-3 years potentially?

Extra slides

Flat space evolution

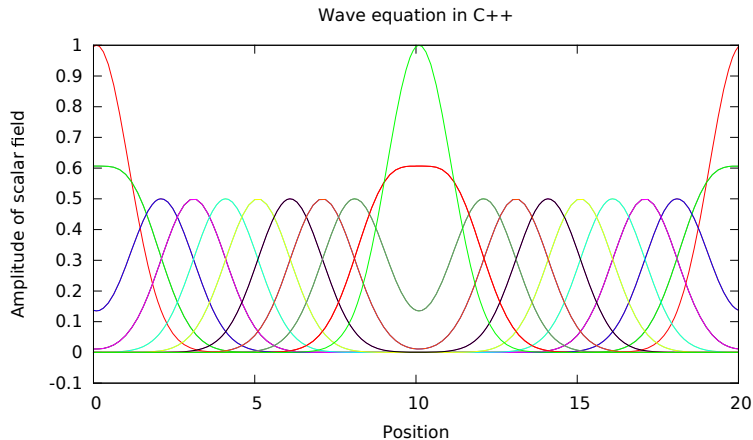


Figure: Gaussian initial conditions, flat spacetime

Flat spacetime error convergence

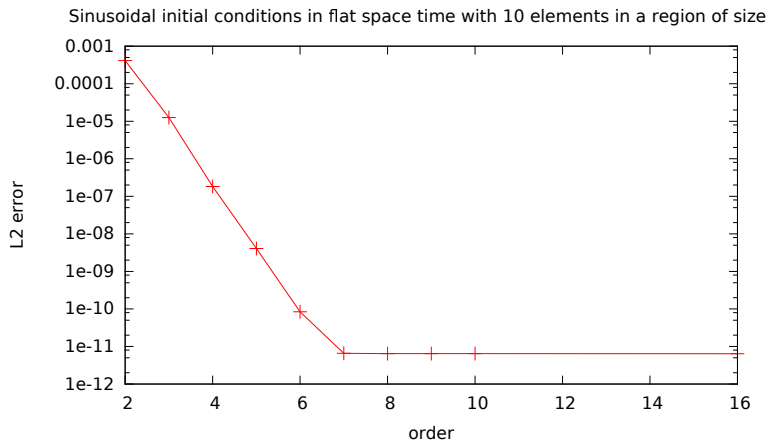
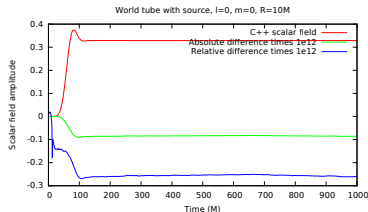
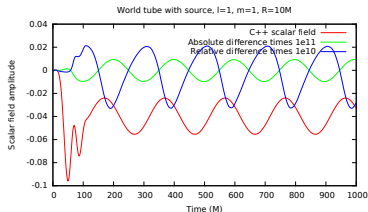


Figure: L_2 error converges exponentially until it hits roundoff noise with DG order for sinusoidal initial conditions with ten elements of size $h = 0.01$.

Circular orbit roundoff error comparison between languages



(a) $l=0$



(b) $l=1$

Figure: Relative and absolute errors are at the roundoff level— 10^{-10} to 10^{-12} . Oscillations do not appear in the $l=0$ mode but appear with the orbital period in the $l=1$ mode.

Precession of the eccentric orbit

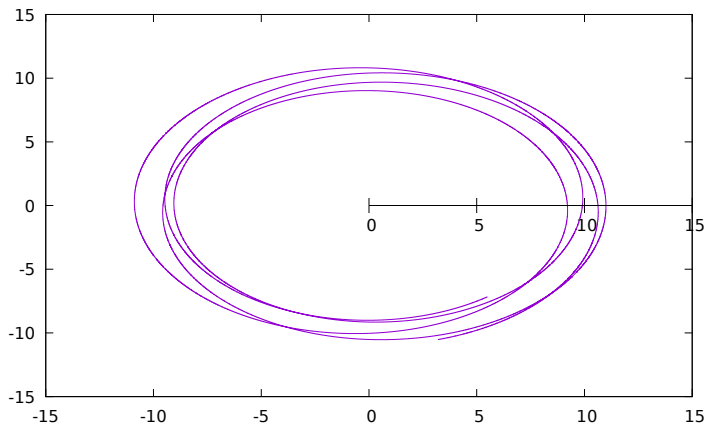


Figure: Precession of the eccentric orbit. $p = 9.9$, $e = 0.0$.

Evolution of the radial self-force for different initial conditions

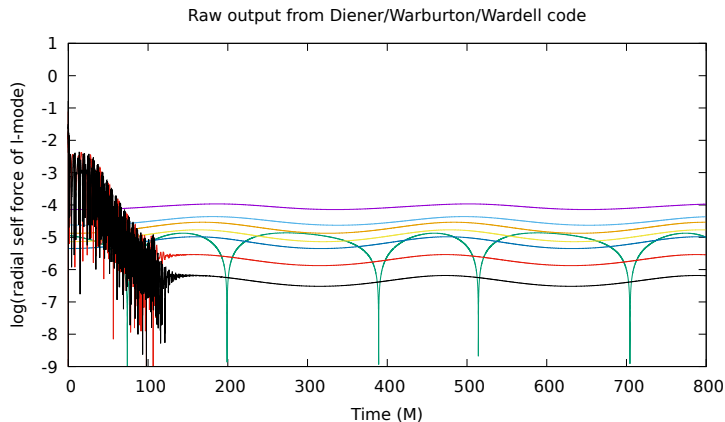
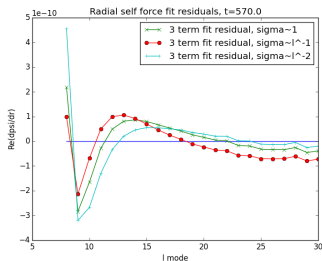
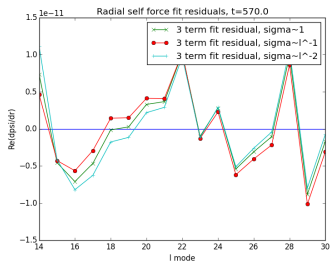


Figure: Low l behavior of the self-force for a given l -mode summed over m

Residuals to the l-mode fit



(a) $l_{\min} = 8$

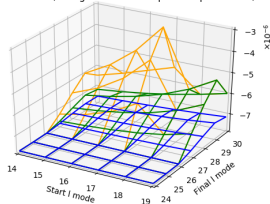


(b) $l_{\min} = 14$

Figure: $l_{\min} = 14$ is a better fit than $l_{\min} = 8$ both because it is less systematically biased and because it has an amplitude an order of magnitude smaller. Both fits end at $l_{\max} = 30$.

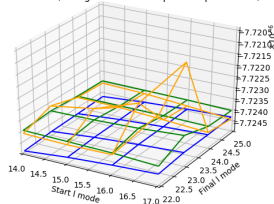
Roundoff noise in F_{inf} at high l_{max}

Total radial self force, using DG error extrapolation per l-mode, $t=635$



(a) Large range

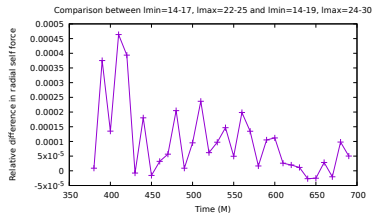
Total radial self force, using DG error extrapolation per l-mode, $t=635$



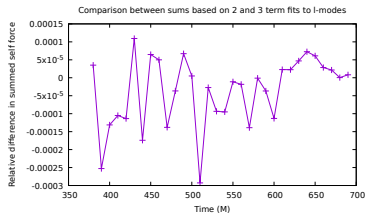
(b) Small range

Figure: $l_{min} = 14$ and $l_{max} = 25$ appear to be good start and stop values. Roundoff noise is evident at higher l .

Error due to l-mode selection, number of terms



(a) large versus small range



(b) 2 versus 3 terms

Figure: Relative errors in both of these effects appear to be at the 10^{-4} level.